

Analytical approach to the quantum-phase transition in the one-dimensional spinless Holstein model

S. Sykora¹, A. Hübsch^{2,3,a}, and K.W. Becker¹

¹ Institut für Theoretische Physik, Technische Universität Dresden, 01062 Dresden, Germany

² Department of Physics, University of California, Davis, CA 95616, USA

³ Max-Planck-Institut für Physik komplexer Systeme, Nöthnitzer Straße 38, 01187 Dresden, Germany

Received 2 November 2005 / Received in final form 23 February 2006

Published online 1st June 2006 – © EDP Sciences, Società Italiana di Fisica, Springer-Verlag 2006

Abstract. We study the one-dimensional Holstein model of spinless fermions interacting with dispersionless phonons by using a recently developed projector-based renormalization method (PRM). At half-filling the system shows a metal-insulator transition to a Peierls distorted state at a critical electron-phonon coupling where both phases are described within the same theoretical framework. The transition is accompanied by a phonon softening at the Brillouin zone boundary and a gap in the electronic spectrum. For different filling, the phonon softening appears away from the Brillouin zone boundary and thus reflects a different type of broken symmetry state.

PACS. 71.10.Fd Lattice fermion models (Hubbard model, etc.) – 71.30.+h Metal-insulator transitions and other electronic transitions

1 Introduction

Systems with strong electron-phonon (EP) interactions have received considerable attention in the last few years, motivated by new findings which suggest a crucial role of the EP coupling in materials with strong electronic correlations. Examples are high-temperature superconductors [1], colossal magnetoresistive manganites [2], or metallic alkaline-doped C₆₀-based compounds [3]. Furthermore, in many quasi one-dimensional materials, such as MX chains, conjugated polymers or organic transfer complexes [4], the kinetic energy of the electrons strongly competes with the EP interaction which tends to establish, e.g., charge-density wave structures.

The so-called spinless Holstein model,

$$\mathcal{H} = -t \sum_{\langle i,j \rangle} (c_i^\dagger c_j + \text{h.c.}) + \omega_0 \sum_i b_i^\dagger b_i + g \sum_i (b_i^\dagger + b_i) n_i, \quad (1)$$

is perhaps the simplest realization of a strongly coupled EP system. It describes the local interaction g at a given lattice site i between the density $n_i = c_i^\dagger c_i$ of electrons and dispersionless phonons with frequency ω_0 . Here, the c_i^\dagger (b_i^\dagger) are fermionic (bosonic) creation operators of electrons (phonons), and $\langle i, j \rangle$ denotes the summation over all neighboring lattice sites i and j .

In the past, a large number of different analytical and numerical methods have been applied to the Holstein model (1). Strong-coupling expansions [5], variational [6] and renormalization group [7,8] approaches, as well as Monte Carlo [5,9] simulations were used to investigate mainly ground-state properties. More recently, exact diagonalization [10] (ED) and density matrix renormalization group (DMRG) [11–13] techniques, and dynamical mean-field theory (DMFT) in conjunction with a numerical renormalization group approach [14] were applied. However, most of these approaches are restricted in their applications, e.g., ED techniques can only handle very small system sizes, DMRG methods require one-dimensional systems, and the DMFT exploits the limit of infinite spatial dimensions. Furthermore, the phononic part of the Hilbert space is infinite even for finite systems so that all numerical approaches require truncation schemes to limit the number of bosonic degrees of freedom, or a numerically expensive systematic reduction of the Hilbert space in the spirit of the DMRG method [15] has to be employed. For these reasons, there is still a clear need of reliable theoretical methods to tackle strongly coupled EP systems in terms of minimal theoretical models. The Holstein model of spinless fermions (1) shows at half-filling a quantum-phase transition from a metallic to an insulating state where both the one-dimensional case and the limit of infinite dimensions have been studied [5,11,14].

Alternative analytical approaches to interacting many-particle systems are offered by methods based

^a e-mail: huebsch@pks.mpg.de

on functional renormalization like the flow equation method [16], the similarity transformation [17], or the projector-based renormalization method (PRM) [18]. So far, these methods have been successfully applied to electron-phonon systems with the aim to study the effective electron-electron interaction [19] or superconductivity [20]. However, the quantum-phase transition in the Holstein model has not yet been studied by this kind of approach.

Recently, we applied the projector-based renormalization method (PRM) [18] to the spinless Holstein model (1) at half-filling [21]. This *analytical* approach does not suffer from the truncation of the phononic Hilbert space so that *all bosonic* degrees of freedom are taken into account. Furthermore, the PRM treatment provides both fermionic and bosonic quasi-particle energies which are *not* directly accessible with other methods. However, the PRM approach of reference [21] was restricted to the metallic phase.

Here, we extend our recent work [21] on the one-dimensional spinless Holstein model (1) where the scope of this paper is twofold: Firstly, we demonstrate that the PRM approach of reference [21] is not restricted to the half-filled case, and that the phonon dispersion relation close to the critical value of the EP coupling reflects the type of the broken symmetry of the insulating phase. Secondly, we derive modified renormalization equations for the half-filled case that enable a dimerization of the system. Thus, we find a *uniform* description for the metallic as well as for the insulating phase of the spinless Holstein model (1) at half-filling. We determine the critical coupling g_c for the metal insulator transition where a careful finite-size scaling is performed. Furthermore, a phonon softening is found for EP couplings close to the critical value g_c which can be understood as a precursor effect of the phase transition.

This paper is organized as follows. In the next section we briefly describe the basic idea of our recently developed PRM approach [18], and discuss metallic solutions of the renormalization equations for different fillings of the electronic band. In particular, we show that the phonon softening close to the critical value g_c of the metal insulator transition reflects the type of the broken symmetry of the insulating phase. In Section 3, we extend the PRM approach of reference [21] to derive an uniform description for the metallic as well as for the insulating phase of the spinless Holstein model (1) at half-filling. Furthermore, in Section 4, the critical coupling g_c for the metal insulator transition is determined, and electronic as well as phononic quasi-particle energies are presented. Finally, we summarize in Section 5.

2 Methodology and metallic solutions

In the PRM approach [18], the final effective Hamiltonian $\tilde{\mathcal{H}} = \lim_{\lambda \rightarrow 0} \mathcal{H}_\lambda$ is obtained by a sequence of unitary transformations,

$$\mathcal{H}_{(\lambda-\Delta\lambda)} = e^{X_{\lambda,\Delta\lambda}} \mathcal{H}_\lambda e^{-X_{\lambda,\Delta\lambda}}, \quad (2)$$

by which transitions between eigenstates of the unperturbed part \mathcal{H}_0 of the Hamiltonian caused by the interaction \mathcal{H}_1 are eliminated in steps. The respective transition energies are used as renormalization parameter λ . The generator $X_{\lambda,\Delta\lambda}$ of the unitary transformation has to be adjusted in such a way so that $\mathcal{H}_{(\lambda-\Delta\lambda)}$ does only contain excitations with energies smaller or equal $(\lambda - \Delta\lambda)$. Interaction with energies larger than $(\lambda - \Delta\lambda)$ are used up to renormalize the parameters of the effective Hamiltonian. Thus, difference equations for the λ dependence of the parameters of the Hamiltonian can be derived which we call renormalization equations.

In reference [21] we have made the following ansatz

$$\mathcal{H}_{0,\lambda} = \sum_k \varepsilon_{k,\lambda} c_k^\dagger c_k + \sum_q \omega_{q,\lambda} b_q^\dagger b_q + E_\lambda, \quad (3)$$

$$\mathcal{H}_{1,\lambda} = \frac{1}{\sqrt{N}} \sum_{k,q} g_{k,q,\lambda} \left(b_q^\dagger c_k^\dagger c_{k+q} + b_q c_{k+q}^\dagger c_k \right) \quad (4)$$

for the renormalized Hamiltonian $\mathcal{H}_\lambda = \mathcal{H}_{0,\lambda} + \mathcal{H}_{1,\lambda}$ after all excitations with energies larger than λ have been eliminated. In the next step, all excitations within the energy shell between $(\lambda - \Delta\lambda)$ and λ have been removed where

$$X_{\lambda,\Delta\lambda} = \frac{1}{\sqrt{N}} \sum_{k,q} B_{k,q,\lambda,\Delta\lambda} \left(b_q^\dagger c_k^\dagger c_{k+q} - b_q c_{k+q}^\dagger c_k \right)$$

has been used as generator of the unitary transformation (2). The coefficients $B_{k,q,\lambda,\Delta\lambda}$ have to be fixed in such a way so that only excitations with energies smaller than $(\lambda - \Delta\lambda)$ contribute to $\mathcal{H}_{(\lambda-\Delta\lambda)}$.

Evaluating equation (2), operator terms that contain four fermionic and bosonic one-particle operators appear. However, to restrict the renormalization scheme to the operators of the renormalization ansatz according equations (3) and (4) we have to perform a factorization approximation,

$$c_k^\dagger c_k c_{k-q}^\dagger c_{k-q} \approx c_k^\dagger c_k \langle c_{k-q}^\dagger c_{k-q} \rangle + \langle c_k^\dagger c_k \rangle c_{k-q}^\dagger c_{k-q} - \langle c_k^\dagger c_k \rangle \langle c_{k-q}^\dagger c_{k-q} \rangle,$$

$$b_q^\dagger b_q c_k^\dagger c_k \approx b_q^\dagger b_q \langle c_k^\dagger c_k \rangle + \langle b_q^\dagger b_q \rangle c_k^\dagger c_k - \langle b_q^\dagger b_q \rangle \langle c_k^\dagger c_k \rangle.$$

Thus, the renormalization equations for $\varepsilon_{k,\lambda}$, $\omega_{q,\lambda}$, E_λ , and $g_{k,q,\lambda}$, that are obtained by comparing the result of the transformation (2) with equations (3) and (4), depend on unknown expectation values $\langle c_k^\dagger c_k \rangle$ and $\langle b_q^\dagger b_q \rangle$. These expectation values are best defined with \mathcal{H}_λ since the renormalization step is done from \mathcal{H}_λ to $\mathcal{H}_{(\lambda-\Delta\lambda)}$. Note that for simplicity in reference [21] the expectation values were evaluated with the unperturbed Hamiltonian $\mathcal{H}_{0,\lambda}$. In contrast, we now neglect the λ dependence of the expectation values and perform the factorization approximation with the full Hamiltonian \mathcal{H} in order to take into account important interaction effects. (A general discussion of the factorization approximation in the PRM can be found in Ref. [22].)

For the evaluation of the expectation values with the full Hamiltonian \mathcal{H} we have to apply the unitary transformations also on operators to exploit $\langle \mathcal{A} \rangle = \langle \mathcal{A}_\lambda \rangle_{\mathcal{H}_\lambda}$. The transformed operator \mathcal{A}_λ is obtained by the sequence (2) of unitary transformations, $\mathcal{A}_{(\lambda-\Delta\lambda)} = e^{X_{\lambda,\Delta\lambda}} \mathcal{A}_\lambda e^{-X_{\lambda,\Delta\lambda}}$. We derive renormalization equations for the fermionic and bosonic one-particle operators, c_k^\dagger and b_q^\dagger , where the same approximations are used as for the Hamiltonian. In this way, equations for the needed expectation values are obtained.

The resulting set of renormalization equations has to be solved self-consistently. The explicit (numerical) evaluation starts from the cutoff $\lambda = \Lambda$ of the original model and proceeds down to $\lambda = 0$. Note that the case $\lambda = 0$ with self-consistently determined expectation values provides the effectively free model $\tilde{\mathcal{H}} = \lim_{\lambda \rightarrow 0} \mathcal{H}_{0,\lambda}$,

$$\tilde{\mathcal{H}} = \sum_k \tilde{\varepsilon}_k c_k^\dagger c_k + \sum_q \tilde{\omega}_q b_q^\dagger b_q + \tilde{E}, \quad (5)$$

we are interested in. Here, we have introduced the renormalized dispersion relations $\tilde{\varepsilon}_k = \lim_{\lambda \rightarrow 0} \varepsilon_{k,\lambda}$ and $\tilde{\omega}_q = \lim_{\lambda \rightarrow 0} \omega_{q,\lambda}$, and the energy shift $\tilde{E} = \lim_{\lambda \rightarrow 0} E_\lambda$.

Here, one might wonder why it is possible to map the Holstein model of spinless fermions onto an effectively *free* system as described above. Of course, before the actual calculations can be started a guess of the form of the final renormalized Hamiltonian $\tilde{\mathcal{H}}$ is needed that can be motivated by the operator terms generated due to the renormalization procedure. Furthermore, the obtained results are a very powerful test of the initial guess: unphysical findings are clear signatures of an insufficient renormalization ansatz. As an example, it will turn out that non-physical negative phonon energies $\tilde{\omega}_q$ are obtained if the electron-phonon coupling g exceeds a critical value. Therefore, we shall later extend ansatz (3), (4) to study both the metallic and the insulating phase of model (1).

Furthermore, it is important to note that the employed factorization approximation is directly related to the renormalization ansatz: only operator structures that are contained in the renormalization ansatz \mathcal{H}_λ can be taken into account without any approximation. All other operators appearing due to the renormalization procedure have to be traced back to those of \mathcal{H}_λ . Here, as already mentioned, we use a factorization approximation for this purpose. Due to the complexity of the renormalization equations it is extremely difficult to estimate the effect of the mentioned factorization approximation on the results. However, in this paper we present two complementary renormalization schemes so that the comparison of the two approaches will provide some information about the effects of the employed factorization approximations (see the discussion in Sect. 4).

In the following we concentrate on the so-called adiabatic case $\omega_0 \ll t$, where we have chosen $\omega_0/t = 0.1$. In panel (a) of Figure 1, the bosonic dispersion relation of an one-dimensional chain at half-filling is shown for different EP couplings g . Due to the coupling between the phononic and electronic degrees of freedom, $\tilde{\omega}_q$ gains some dispersion. In particular, a phonon softening appears at

the Brillouin-zone boundary if g is only slightly smaller than the critical value $g_c \approx 0.31t$ of the EP coupling. However, if the EP coupling g exceeds the critical value g_c we obtain non-physical negative phonon energies. Therefore, the solutions of the renormalization equations from reference [21] can only describe the metallic phase and break down at the phase transition.

As already mentioned above, in the present calculation an improved scheme for the evaluation of the expectation values has been used. However, the same critical value $g_c \approx 0.31t$ for the metal-insulator transition was also found in reference [21] where all expectation values had been evaluated using the unperturbed part $\mathcal{H}_{0,\lambda}$ of the λ dependent Hamiltonian and not using the full Hamiltonian \mathcal{H} .

Note that the critical EP coupling $g_c \approx 0.31t$ obtained from the vanishing phonon mode at the Brillouin-zone boundary is significantly larger than the DMRG value of $g_c \approx 0.28t$ [11,13]. This difference can be understood as follows: our renormalization scheme as presented in this section starts from a description particularly suitable for the metallic phase as represented by the final Hamiltonian $\tilde{\mathcal{H}}$. As discussed above, a factorization approximation has been employed so that fluctuations are suppressed. However, these additional fluctuations would enhance the phonon softening and, therefore, tend to destabilize the metallic phase. Thus, the realistic critical value g_c of the electron-phonon coupling is smaller than the result we have obtained by the PRM approach as presented above. Note that the situation will change for the modified renormalization scheme of Section 3.

Even though only the case of half-filling has been discussed in reference [21], the same PRM approach can also be applied to different fillings without any modifications. Panel (b) of Figure 1 shows bosonic dispersion relations for an one-dimensional chain at filling 1/3 for different EP couplings. Similar to the half-filled case, we obtain a phonon softening for EP couplings g close to a critical value of $g_c \approx 0.5t$, and negative phonon energies are observed for $g > g_c$. However, in contrast to the half-filled case, the phonon softening appears at $2k_F = 2\pi/3$ and not at the Brillouin-zone boundary (where k_F denotes the Fermi momentum). Consequently, as expected for a one-dimensional fermionic system, the broken symmetry of the insulating phase *strongly* depends on the filling of the electronic band.

Figure 2 shows the critical values g_c of the EP coupling as function of the electronic band filling. Here, two aspects of the results are important to be noticed: (i) the critical value g_c has a minimum at half-filling which is connected with the highest stability of the insulating phase; (ii) the form of the curve in Figure 2 reflects the particle-hole symmetry of the model (1).

Above we have argued that the phonon softening is a precursor effect of the metal-insulation transition in the Holstein model. However, in the anti-adiabatic limit of the model where $t \ll \omega_0$ holds we do obtain the opposite behavior: a phonon stiffening occurs in the metallic phase if we increase the electron-phonon coupling g .

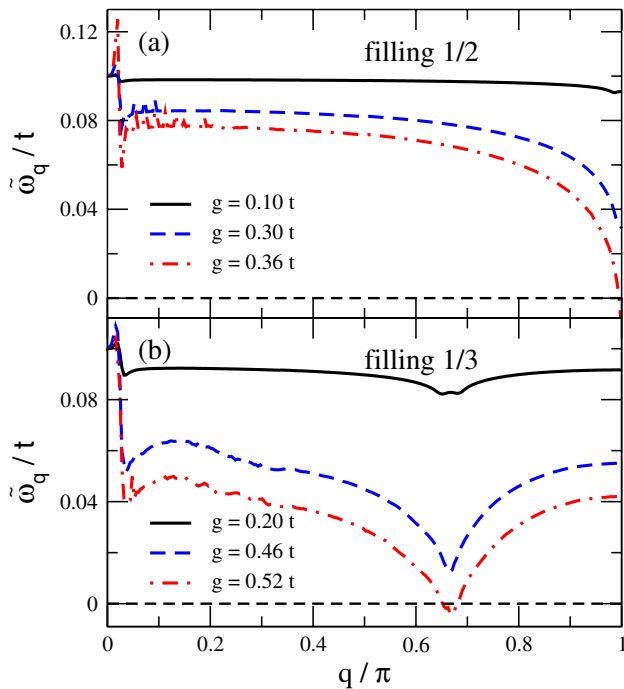


Fig. 1. (Color online) Bosonic quasi-particle energies of a chain with 500 lattice sites for different EP couplings g obtained from the renormalization equations without a symmetry breaking term. Note the unphysical jumps at small q values which are due to the factorization approximation of higher order renormalization processes. For details see the discussion in reference [21].

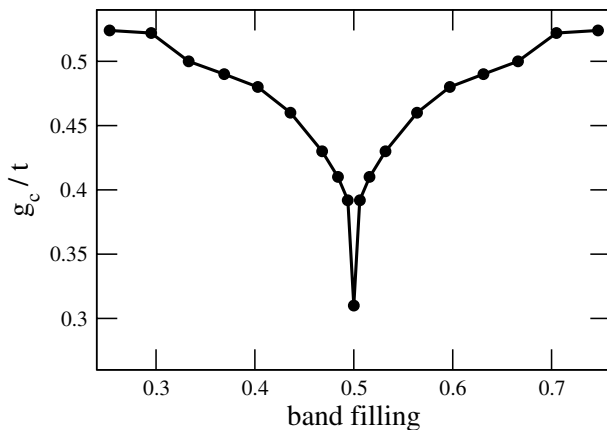


Fig. 2. Critical value g_c of the EP coupling as a function of the electronic band filling for a chain with 500 lattice sites. The value $g_c \approx 0.31t$ for the half-filled case agrees perfectly with the result of reference [21] where a simpler scheme for the evaluation of the expectation values has been used.

This finding corresponds to the anti-adiabatic limit of spin systems where also no phonon softening occurs for fast phonons [23]. Unfortunately, in this work the metal-insulator transition itself can not be studied in the anti-adiabatic limit because the presented PRM approach has no stable solutions for $t \ll g$.

3 Uniform description of metallic and insulating phases at half-filling

In this section we want to extend our PRM approach to find an uniform description for the metallic as well as for the insulating phase of the spinless Holstein model (1). In the following, we concentrate on the case of half-filling because the broken symmetry of the insulating phase depends strongly on the filling of the electronic band as discussed above.

We have already mentioned that the PRM approach as discussed in Section 2 breaks down for strong EP couplings. In this case a long-range charge density wave order occurs, and electrons and ions are shifted from their symmetric positions. To describe such a state with a broken symmetry in the framework of the PRM the ansatz for \mathcal{H}_λ must contain suited order parameters [20]. In the case of the half-filled Holstein model, one has to take into account that the unit cell of the system is doubled in the case of a dimerized insulating ground-state. Therefore, we consider the Hamiltonian in a reduced Brillouin zone and introduce appropriate symmetry breaking terms in our renormalization ansatz. Thus, the renormalized Hamiltonian $\mathcal{H}_\lambda = \mathcal{H}_{0,\lambda} + \mathcal{H}_{1,\lambda}$ reads

$$\begin{aligned} \mathcal{H}_{0,\lambda} &= \sum_{k>0,\alpha} \varepsilon_{\alpha,k,\lambda} c_{\alpha,k}^\dagger c_{\alpha,k} + \sum_{q>0,\gamma} \omega_{\gamma,q,\lambda} b_{\gamma,q}^\dagger b_{\gamma,q} + E_\lambda \\ &+ \sum_k \Delta_{k,\lambda}^c (c_{0,k}^\dagger c_{1,k} + \text{h.c.}) + \sqrt{N} \Delta_\lambda^b (b_{1,Q}^\dagger + \text{h.c.}) \quad (6) \\ \mathcal{H}_{1,\lambda} &= \frac{1}{\sqrt{N}} \sum_{\substack{k,q>0 \\ \alpha,\beta,\gamma}} g_{k,q,\lambda}^{\alpha,\beta,\gamma} \left\{ \delta(b_{\gamma,q}^\dagger) \delta(c_{\alpha,k}^\dagger c_{\beta,k+q}) + \text{h.c.} \right\} \quad (7) \end{aligned}$$

after all excitations with energies larger than λ have been integrated out. Here, due to the usage of the reduced Brillouin zone, both the fermionic and bosonic one-particle operators as well as the model parameters have additional band indices, $\alpha, \beta, \gamma = 0, 1$. Furthermore, the definitions $\delta A = A - \langle A \rangle$ and $Q = \pi/a$ are used in equation (7). Note, however, that equation (6) is restricted to the one-dimensional case at half-filling but could be easily extended: for higher dimensions the term with the order parameter Δ_λ^b has to take into account all \mathbf{Q} values of the Brillouin zone boundary. To describe the insulating phase away from half-filling one has to adjust the order parameters because the broken symmetry type strongly depends on the filling as discussed above.

To derive the renormalization equations we consider the renormalization step from λ to $(\lambda - \Delta\lambda)$. At first we perform a rotation in the fermionic subspace and a translation to new ionic equilibrium positions so that $\mathcal{H}_{0,\lambda}$ is diagonalized,

$$\begin{aligned} \mathcal{H}_{0,\lambda} &= \sum_{k>0} \sum_{\alpha} \varepsilon_{\alpha,k,\lambda}^C C_{\alpha,k,\lambda}^\dagger C_{\alpha,k,\lambda} \\ &+ \sum_{q>0} \sum_{\gamma} \omega_{\gamma,q,\lambda}^B B_{\gamma,q,\lambda}^\dagger B_{\gamma,q,\lambda} - E_\lambda. \quad (8) \end{aligned}$$

Next we rewrite $\mathcal{H}_{1,\lambda}$ in terms of the new fermionic and bosonic creation and annihilation operators, $C_{\alpha,k,\lambda}^{(\dagger)}$ and $B_{\gamma,q,\lambda}^{(\dagger)}$ which we have introduced to diagonalize $\mathcal{H}_{0,\lambda}$. Finally, we have to evaluate (2) to derive the renormalization equations for the parameters of \mathcal{H}_λ . Here the ansatz

$$X_{\lambda,\Delta\lambda} = \frac{1}{\sqrt{N}} \sum_{k,q} \sum_{\alpha,\beta,\gamma} A_{k,q,\lambda,\Delta\lambda}^{\alpha,\beta,\gamma} \times \left\{ \delta B_{\gamma,q}^\dagger \delta (C_{k,\lambda}^\dagger C_{\beta,k+q,\lambda}) - \text{h.c.} \right\}$$

is used for the generator of the unitary transformation (2). The coefficients $A_{k,q,\lambda,\Delta\lambda}^{\alpha,\beta,\gamma}$ have to be fixed in such a way so that only excitations with energies smaller than $(\lambda - \Delta\lambda)$ contribute to $\mathcal{H}_{1,(\lambda-\Delta\lambda)}$. The renormalization equations for the parameters $\epsilon_{k,\lambda}$, $\Delta_{k,\lambda}^c$, $\omega_{\gamma,q,\lambda}$, Δ_λ^b , and $g_{k,q,\lambda}^{\alpha,\beta,\gamma}$ are obtained by comparison with (6), (7) after the creation and annihilation operators $C_{\alpha,k,\lambda}^{(\dagger)}$, $B_{\gamma,q,\lambda}^{(\dagger)}$ have been transformed back to the original operators $c_{\alpha,k}^{(\dagger)}$, $b_{\gamma,q}^{(\dagger)}$. The actual calculations are done in close analogy to reference [21].

As already discussed in Section 2, in order to evaluate equation (2), an additional factorization approximation must be employed where only operators of the structure of those of (6) and (7) are kept. At this point it is important to notice that this factorization approximation is performed in the framework of the reduced Brillouin zone. Therefore, in comparison to the PRM scheme of Section 2, additional terms occur for non-zero order parameters $\Delta_{k,\lambda}^c$ and Δ_λ^b . Due to the factorization approximation, the final renormalization equations still depend on unknown expectation values. As already discussed in Section 2, these expectation values were evaluated with the full Hamiltonian \mathcal{H} in order to take into account important interaction effects. Therefore, we again must apply the sequence (2) of unitary transformations to operators, $\mathcal{A}_{(\lambda-\Delta\lambda)} = e^{X_{\lambda,\Delta\lambda}} \mathcal{A}_\lambda e^{-X_{\lambda,\Delta\lambda}}$ to exploit $\langle \mathcal{A} \rangle = \langle \mathcal{A}_\lambda \rangle_{\mathcal{H}_\lambda}$. As in Section 2, this procedure is performed for the fermionic and bosonic one-particle operators, $c_{\alpha,k}^\dagger$ and $b_{\gamma,q}^\dagger$, where the same approximations are used as for the Hamiltonian. Thus, we easily obtain equations for the needed expectation values. The resulting set of renormalization equations is solved numerically where the equations for the expectation values are taken into account due to a self-consistency loop.

The case $\lambda = 0$ with self-consistently determined expectation values provides again an effectively free model $\tilde{\mathcal{H}} = \lim_{\lambda \rightarrow 0} \mathcal{H}_\lambda = \lim_{\lambda \rightarrow 0} \mathcal{H}_{0,\lambda}$ which reads

$$\tilde{\mathcal{H}} = \sum_{k>0,\alpha} \tilde{\epsilon}_{\alpha,k} c_{\alpha,k}^\dagger c_{\alpha,k} + \sum_{k>0} \tilde{\Delta}_k^c (c_{0,k}^\dagger c_{1,k} + \text{h.c.}) + \sum_{q>0,\gamma} \tilde{\omega}_{\gamma,q} b_{\gamma,q}^\dagger b_{\gamma,q} + \sqrt{N} \tilde{\Delta}^b (b_{1,Q}^\dagger + b_{1,Q}) - \tilde{E} \quad (9)$$

where $\tilde{\epsilon}_{\alpha,k} = \lim_{\lambda \rightarrow 0} \epsilon_{\alpha,k,\lambda}$, $\tilde{\Delta}_k^c = \lim_{\lambda \rightarrow 0} \Delta_{k,\lambda}^c$, $\tilde{\omega}_{\gamma,q} = \lim_{\lambda \rightarrow 0} \omega_{\gamma,q,\lambda}$, and $\tilde{\Delta}^b = \lim_{\lambda \rightarrow 0} \Delta_\lambda^b$. Note that all excitations from $\mathcal{H}_{1,\lambda}$ were used up to renormalize the param-

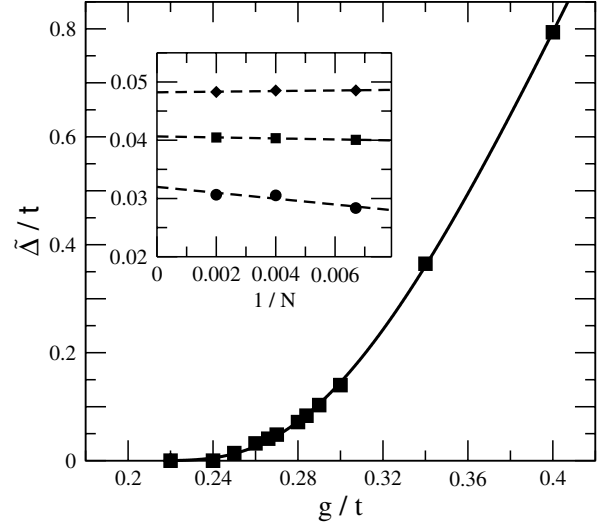


Fig. 3. Gap in the electronic excitation spectrum for the infinite chain. The solid line is a Kosterlitz-Thouless fit of the form $\tilde{\Delta}/t = \frac{15.240}{\sqrt{(g/t)^2 - (0.195)^2}} \exp\left[-\frac{1.400}{\sqrt{(g/t)^2 - (0.195)^2}}\right]$. The inset shows the finite-size scaling for g values of 0.26t (circles), 0.266t (squares), and 0.27t (diamonds).

eters of $\tilde{\mathcal{H}}_0$. The expectation values are also calculated in the limit $\lambda \rightarrow 0$ and can be easily determined from $\langle A \rangle_{\mathcal{H}} = \langle A_\lambda \rangle_{\mathcal{H}_\lambda} = \langle (\lim_{\lambda \rightarrow 0} A_\lambda) \rangle_{\tilde{\mathcal{H}}}$ because $\tilde{\mathcal{H}}$ is a free model.

Before we present results in Section 4, we want to compare the two different renormalization schemes discussed above in more detail. As already mentioned, the approach of Section 2 is based on a renormalization ansatz in particular suitable for the metallic phase of the system. In contrast, the renormalization scheme as discussed in the present section starts from a dimerized system so that this approach provides a description of the system particularly adapted to the insulating phase. Thus, both renormalization schemes are complementary approaches, and opposite fluctuations are suppressed due to the employed factorization approximations: the suppressed fluctuations of the renormalization scheme of Section 2 *destabilize* the metallic phase. In contrast, it will be shown that the neglected fluctuations of the approach of Section 3 *favor* the same phase.

On the other hand, the two renormalization schemes are not only complementary in their starting points but also closely related: the renormalization scheme as discussed in the present section *exactly* matches the approach of Section 2 if the gap parameters $\Delta_{k,\lambda}^c$ and Δ_λ^b vanish for all λ values. Thus, finite excitation gaps are only obtained from the renormalization scheme of this section if the insulating (i.e. gapped) phase has a lower free energy than the metallic solution as discussed in Section 2. Note that in actual calculations the PRM approach of this section *always* leads to a free energy smaller than the one obtained from the scheme discussed in Section 2.

4 Results

In the following, we first show that the PRM treatment can be used to investigate the Peierls transition of the one-dimensional spinless Holstein model (1) at half-filling. In particular, our analytical approach provides a theoretical description for the metallic as well as for the insulating phase, and we compare our results with DMRG calculations [11, 13].

In order to determine g_c we perform a careful finite-size scaling as shown for some g values in the inset of Figure 3 where a linear regression is applied to extrapolate our results to infinite system size. Note, however, that the finite size scaling of our PRM approach is affected by two different effects: long-range fluctuations are suppressed by the finite cluster size as well as by the used factorization approximation so that a rather unusual dependence on the system size is found. In Figure 3 the electronic excitation gap $\tilde{\Delta}$ for infinite system size, as found from the opening of a gap in the quasi-particle energy $\tilde{\varepsilon}_k$ (see text below), is plotted as function of the EP coupling g . A closer inspection of the data shows that an insulating phase with a finite excitation gap is obtained for g values larger than the critical EP coupling $g_c \approx 0.24t$. A comparison with the critical value $g_c \approx 0.28t$ obtained from DMRG calculations [11, 13] shows that the critical values from the PRM approach of Section 3 might be somewhat too small.

In particular, the critical coupling $g_c \approx 0.24t$ obtained from the opening of the gap in $\tilde{\varepsilon}_k$ is significantly smaller than the g_c value of $\approx 0.31t$ which was found from the vanishing of the phonon mode at the Brillouin zone boundary in the metallic solution of Section 2. Instead, one would expect that both the gap in $\tilde{\varepsilon}_k$ and the vanishing of $\tilde{\omega}_q$ should occur at the same g_c value. This inconsistency can be understood from the different nature of the factorization approximations employed in the two PRM approaches presented here: as discussed above, the due to the factorization approximation suppressed fluctuations tend to destabilize the suggested phase of the renormalization ansatz. Therefore, the neglected fluctuations of the two presented PRM approaches have opposite characters: the stability of the metallic phase is overestimated by the scheme of Section 2 whereas the approach of Section 3 favors the insulating phase, and the different values of the critical coupling exactly reflect the different nature of the two PRM approaches. Thus, both approaches (and both ways to determine g_c) would be consistent with each other if additional fluctuation could be taken into account, and one would expect a common result for g_c between $0.24t$ and $0.31t$. This would be in good agreement with the DMRG value of $g_c \approx 0.28t$ [11, 13].

Another way to determine g_c might be given by the assumption that a marginal relevant interaction in a renormalization group treatment causes the phase transition in the Holstein model. Corresponding to reference [24], the gap $\tilde{\Delta}$ should in this case grow for $g > g_c$ as $\exp[-a/g - g_c]$, where a is some numerical constant. Such a function fits our data very well, and a critical value of $g_c = 0.166t$ would result in this way which seems to be questionable small. On the other hand, we could

also assume that the metal-insulator transition might be of Kosterlitz-Thouless type [25] as found for the anti-adiabatic limit of spin-Peierls chains [26]. As one can see in Figure 3, the Kosterlitz-Thouless gap formula [27, 26], $\tilde{\Delta} \propto (g^2 - g_c^2)^{-0.5} \exp(-a/\sqrt{g^2 - g_c^2})$, also fits our data and leads to a critical value of $g_c = 0.195t$. However, such a small value contradicts other finding of our calculations: as discussed above, the phonon softening at the Brillouin-zone boundary is a clear signature of the occurring phase transition, and the smallest phonon energies should be obtained for g_c . This test provides clear evidence for a critical value of $g_c \approx 0.24t$.

The quasi-particle energies are also directly accessible: after the renormalization equations were solved self-consistently the electronic and phononic quasi-particle energies of the system, $\tilde{\varepsilon}_k$ and $\tilde{\omega}_q$, respectively, are given by the limit $\lambda \rightarrow 0$ of the parameters $\varepsilon_{\alpha,k,\lambda}^C$ and $\omega_{\gamma,q,\lambda}^B$ of the unperturbed part $\mathcal{H}_{0,\lambda}$ of the Hamiltonian in its diagonalized form (8).

In Figure 4 the renormalized one-particle energies (which have to be interpreted as the quasi-particle energies of the full system) are shown for different values of the EP coupling g . As one can see from the upper panel, the electronic one-particle energies depend only slightly on g as long as g is smaller than the critical value $g_c \approx 0.24t$. If the EP coupling g is further increased a gap Δ opens at the Fermi energy so that the system becomes an insulator. Remember that the gap $\tilde{\Delta}$ has been used as order parameter to determine the critical EP coupling g_c of the metal-insulator transition (see Fig. 3). The lower panel of Figure 4 shows the results for the phononic one-particle energies $\tilde{\omega}_q$. One can see that $\tilde{\omega}_q$ gains dispersion due to the coupling g between the electronic and phononic degrees of freedom. In particular, the phonon mode at momentum $2k_F = \pi$, i.e. at the Brillouin-zone boundary, becomes soft if the EP coupling is increased up to $g_c \approx 0.24t$. However, in contrast to the metallic solution of Section 2 $\tilde{\omega}_q$ at $2k_F$ always remains positive though it is very small. Note that for g values larger than g_c $\tilde{\omega}_q$ increases again. This phonon softening at the phase transition has to be interpreted as a lattice instability which leads to the formation of the insulating Peierls state for $g > g_c$. The phase transition is associated with a shift of the ionic equilibrium positions. A lattice stiffening occurs if g is further increased to values much larger than the critical value $g_c \approx 0.24t$.

5 Summary

In this paper, the recently developed PRM approach has been applied to the one-dimensional Holstein model (1) of spinless fermions interacting with dispersion-less phonons. In extension to our earlier work [21], here, we have improved the scheme for the evaluation of expectation values, and have discussed the metal-insulator transition of the model for different fillings of the electronic band. Furthermore, for the half-filled Holstein model we have derived an uniform description for the metallic as well as for the insulating phase.

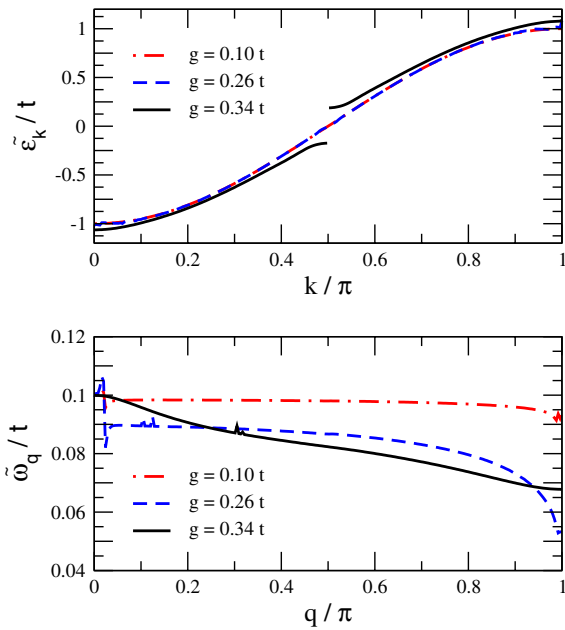


Fig. 4. (Color online) Fermionic (upper panel) and bosonic (lower panel) quasi-particle energies of a chain with 500 lattice sites for different EP couplings g .

We have shown that the renormalized phonon energies gain a momentum dependence due to the EP coupling. In particular, for half-filling a phonon softening at $2k_F$ appears if the EP coupling is close to the critical value of the metal-insulator transition. Therefore, the broken symmetry of the insulating phase strongly depends on the filling of the electronic band. The critical value of the metal-insulator transition also depends on the band filling, where the insulating phase has at half-filling the highest stability.

The PRM approach of reference [21] breaks down if the EP coupling exceeds the critical value of the metal-insulator transition. Here, we have extended our PRM approach to enable symmetry broken insulating states. Thus, we derived a *uniform* description for the metal as well as for the insulating phase (which is restricted to the half-filled case of the Holstein model). Here, we have used this extended analytical framework to study the phase transition in more detail. We have determined the critical value of the EP coupling for the metal-insulator transition. Furthermore, we have shown the opening of the excitation gap in the electronic quasi-particle energies, and the lattice stiffening for EP couplings larger than the critical value.

We would like to acknowledge helpful discussions with T.M. Bryant. This work was supported by the DFG through the research program SFB 463 and under Grant No. HU 993/1-1,

and by the US Department of Energy, Division of Materials Research, Office of Basic Energy Science.

References

1. A. Lanzara et al., *Nature* **412**, 510 (2001)
2. A.J. Millis, P.B. Littlewood, B.I. Shraiman, *Phys. Rev. Lett.* **74**, 5144 (1995)
3. O. Gunnarsson, *Rev. Mod. Phys.* **69**, 575 (1997)
4. A.R. Bishop, B.I. Swanson, *Los Alamos Science* **21**, 133 (1993); N. Tsuda, K. Nasu, A. Yanese, K. Siratori, *Electronic Conduction in Oxides* (Springer-Verlag, Berlin, 1990); *Organic Conductors*, edited by J.-P. Farges (Marcel Dekker, New York, 1994)
5. J.E. Hirsch, E. Fradkin, *Phys. Rev. B* **27**, 4302 (1983)
6. H. Zheng, D. Feinberg, M. Avignon, *Phys. Rev. B* **39**, 9405 (1989)
7. L.G. Caron, C. Bourbonnais, *Phys. Rev. B* **29**, 4230 (1984)
8. G. Benfatto, G. Gallovotti, J.L. Lebowitz, *Helv. Phys. Acta* **68**, 312 (1995)
9. R.H. McKenzie, C.J. Hamer, D.W. Murray, *Phys. Rev. B* **53**, 9676 (1996)
10. A. Weiße, H. Fehske, *Phys. Rev. B* **58**, 13526 (1998); H. Fehske, M. Holicki, A. Weiße, *Advances in Solid State Physics* **40**, 235 (2000)
11. R.J. Bursill, R.H. McKenzie, C.J. Hamer, *Phys. Rev. Lett.* **80**, 5607 (1998)
12. E. Jeckelmann, C. Zhang, S.R. White, *Phys. Rev. B* **60**, 7950 (1999)
13. H. Fehske, G. Wellein, G. Hager, A. Weiße, K.W. Becker, A.R. Bishop, *Physica B* **359–361**, 699 (2005)
14. D. Meyer, A.C. Hewson, R. Bulla, *Phys. Rev. Lett.* **89**, 196401 (2002)
15. C. Zhang, E. Jeckelmann, S.R. White, *Phys. Rev. B* **80**, 2661 (1998)
16. F.J. Wegner, *Ann. Physik (Leipzig)* **3**, 77 (1994)
17. S.D. Glazek, K.G. Wilson, *Phys. Rev. D* **48**, 5863 (1993); *ibid.* **49**, 4214 (1994)
18. K.W. Becker, A. Hübsch, T. Sommer, *Phys. Rev. B* **66**, 235115 (2002)
19. P. Lenz, F. Wegner, *Nucl. Phys. B* **482**, 693 (1996)
20. A. Hübsch, K.W. Becker, *Eur. Phys. J. B* **33**, 391 (2003)
21. S. Sykora, A. Hübsch, K.W. Becker, G. Wellein, H. Fehske, *Phys. Rev. B* **71**, 045112 (2005)
22. A. Hübsch, K.W. Becker, *Phys. Rev. B* **71**, 155116 (2005)
23. See, for example, G.S. Uhrig, *Phys. Rev. B* **57**, R14004 (1998); R. Citro, E. Orignac, T. Giamarchi, *Phys. Rev. B* **72**, 024434 (2005)
24. S.R. White, I. Affleck, *Phys. Rev. B* **54**, 9862 (1996)
25. J.M. Kosterlitz, J.M. Thouless, *J. Phys. C* **6**, 1181 (1973)
26. L.G. Caron, S. Moukouri, *Phys. Rev. Lett.* **76**, 4050 (1996)
27. R.J. Baxter, *J. Phys. C* **6**, L94 (1973)